Stem Cell Research (2014) 12, 387–399

Available online at www.sciencedirect.com

ScienceDirect

www.elsevier.com/locate/scr

# Selective neuronal differentiation of neural stem cells induced by nanosecond microplasma agitation☆

Z. Xiong[a,e,1], S. Zhao[b,1], X. Mao[b,1], X. Lu[a,*], G. He[b,*], G. Yang[b], M. Chen[b], M. Ishaq[c], K. Ostrikov[c,d,**]

[a] State Key Laboratory of Advanced Electromagnetic Engineering and Technology, Huazhong University of Science and Technology, Wuhan, Hubei 430030, PR China
[b] The Genetic Engineering International Cooperation Base of Chinese Ministry of Science and Technology, Chinese National Center of Plant Gene Research (Wuhan) HUST Part, College of Life Science and Technology, Huazhong University of Science & Technology (HUST), Wuhan 430074, PR China
[c] Transformational Biology TCP and Plasma Nanoscience Laboratories, CSIRO Materials Science and Engineering, P. O. Box 218, Lindfield, NSW 2070, Australia
[d] Brain Dynamics Group, Complex Systems, School of Physics, Faculty of Science, The University of Sydney, Sydney, NSW 2006, Australia
[e] Department of Chemical and Biomolecular Engineering, University of California, Berkeley, CA 94720, USA

Received 15 June 2013; received in revised form 2 November 2013; accepted 5 November 2013
Available online 13 November 2013

**Abstract** An essential step for therapeutic and research applications of stem cells is their ability to differentiate into specific cell types. Neuronal cells are of great interest for medical treatment of neurodegenerative diseases and traumatic injuries of central nervous system (CNS), but efforts to produce these cells have been met with only modest success. In an attempt of finding new approaches, atmospheric-pressure room-temperature microplasma jets (MPJs) are shown to effectively direct *in vitro* differentiation of neural stem cells (NSCs) predominantly into neuronal lineage. Murine neural stem cells (C17.2-NSCs) treated with MPJs exhibit rapid proliferation and differentiation with longer neurites and cell bodies eventually forming neuronal networks. MPJs regulate ~75% of NSCs to differentiate into neurons, which is a higher efficiency compared to common protein- and growth factors-based differentiation. NSCs exposure to quantized and transient (~150 ns) micro-plasma bullets

*Abbreviations:* CNS, central nervous system; MPJs, microplasma jets; NSCs, neural stem cells; NO, nitric oxide; qRT-PCR, quantitative real-time PCR; NDs, neurological diseases; ROS, reactive oxygen species; RNS, reactive nitrogen species; UV, ultraviolet; GFAP, glial fibrillary acidic protein; APC, adenomatous polyposis coli; OEC, olfactory ensheathing cell; FBS, fetal bovine serum; HS, horse serum; DMEM, Dulbecco's modified Eagle medium; SDS-PAGE, sodium dodecyl sulfate-polyacryl amide gel electrophoresis; TH, Tyrosine Hydroxylase.



* Corresponding authors at: Huazhong University of Science and Technology, Wuhan, Hubei 430030, PR China.
** Corresponding author at: CSIRO Materials Science and Engineering, P.O. Box 218, Lindfield, NSW 2070, Australia.
*E-mail addresses:* luxinpei@hotmail.com (X. Lu), hegy@hust.edu.cn (G. He), kostya.ostrikov@csiro.au (K. Ostrikov).
[1] These authors contributed equally to this work.

1873-5061/$ - see front matter 
http://dx.doi.org/10.1016/j.scr.2013.11.003

up-regulates expression of different cell lineage markers as β-Tubulin III (for neurons) and O4 (for oligodendrocytes), while the expression of GFAP (for astrocytes) remains unchanged, as evidenced by quantitative PCR, immunofluorescence microscopy and Western Blot assay. It is shown that the plasma-increased nitric oxide (NO) production is a factor in the fate choice and differentiation of NSCs followed by axonal growth. The differentiated NSC cells matured and produced mostly cholinergic and motor neuronal progeny. It is also demonstrated that exposure of primary rat NSCs to the microplasma leads to quite similar differentiation effects. This suggests that the observed effect may potentially be generic and applicable to other types of neural progenitor cells. The application of this new *in vitro* strategy to selectively differentiate NSCs into neurons represents a step towards reproducible and efficient production of the desired NSC derivatives.


## Introduction

Neural stem cells (NSCs), with their ability to differentiate into mature cell types provide an unlimited source of 'raw material' for regenerative medicine therapies of many incurable diseases (Bergmann and Frisén, 2013). However, applications of NSCs in regenerative medicine are hampered by the lack of insufficient methods for directed differentiation. Cell lineages derived from NSCs including neurons, oligodendrocytes and astrocytes are of significant interest for many applications in regenerative medicine and medical treatments of traumatic injuries of neural system (Hernández-Benítez et al., 2012; Rossi and Cattaneo, 2002).

Neurological diseases (NDs) generally affect the central, peripheral, and vegetative nervous systems. They mainly effect by functional disruption of feelings, motions, and consciousness. NDs include brain trauma, spinal cord injury, crania-cerebral, Alzheimer's and Parkinson's diseases (Bjorklund and Lindvall, 2000; Breunig et al., 2011; Grois et al., 1998; McKay, 1997; Rodriguez et al., 2009; Sleeper et al., 2002). Presently available treatments of nervous system diseases include: 1) traditional drug therapy in which drugs are used as a source of nutrition for the recovery of damaged nerve cells; 2) gene therapy; and 3) transplantation of central nervous tissues (Sunde and Zimmer, 1981). However, the progress in approaches based on nervous tissue transplantation is quite limited, in part due to ethics regulations related to embryonic brain. Recently, a new method based on neural stem cells isolation and cloning has been employed as a successful *in vitro* strategy for the treatment of nervous system diseases (Reynolds and Weiss, 1992; Temple, 2001). NSCs exhibit the potency to differentiate into the main phenotypes in the nervous system (*e.g.*, cortical neurons) and as such show great potential to resolve neurological and neurotraumatic disorders without raising ethics issues (Breunig et al., 2011).

The key purpose of cultivating neural stem cells *in vitro* is to control and enhance the cell fate commitment, differentiation into well-resolved cell types, proliferation, and migration. Therapeutic use of NSC differentiation into neurons for tissue transplantation to treat nervous system disorders is an important hallmark of stem cell research (Temple, 2001). This method is considered one of the most promising therapies for neurodegenerative and neurotraumatic diseases. Previous reports have shown that cytokines, chemicals, Chinese medicines, selected proteins, hormones, electrical stimulation, and local environmental factors could affect the differentiation of NSCs (Boyer et al., 2005; Chambers et al., 2003; Flanagan et al., 2006; Hwang et al., 2004; Okada et al., 2004; J.-H. Wang et al., 2006; J. Wang et al., 2006). For example, excessive nephroblastoma gene expression may enhance NSCs proliferation and differentiation (Shi et al., 2006). Carbon nanotube ropes with electrical stimulation may also stimulate the differentiation of NSCs into the neuronal lineage (Huang et al., 2012). Olfactory ensheathing cell (OEC) conditioned medium was found to promote axonal regeneration and functional recovery after transplantation (Barnett, 2004; Pellitteri et al., 2009). However, these biochemical (*e.g.*, based on the presentation of differentiation factors in the medium) and more recent, nanotechnology-based methods of NSCs differentiation have quite significant drawbacks including chemical toxicity, insufficient selectivity of cell-type-specific differentiation, glial scar formation after transplantation, and several others (Rossi and Cattaneo, 2002). Therefore, there is a strong demand for new techniques for cell-type-specific, efficient, and safe NSC differentiation.

Non-thermal (non-equilibrium) atmospheric-pressure plasmas (Ostrikov et al., 2013), including atmospheric-pressure room-temperature microplasma jets (MPJs) of interest here have recently been very effective in cancer therapy, blood coagulation, root canal treatment, wound healing, antimicrobial and other applications (Keidar et al., 2011; Kim et al., 2010; Kolb et al., 2008; Laroussi, 1996; Lloyd et al., 2010). There are two most common types of the atmospheric-pressure plasmas that are used in biomedical treatments, namely "direct" and "indirect" plasma devices. In the first type of devices, a living tissue acts as an electrode, while the second type of devices, which include the MPJs, produces the plasma plumes that emerge outside the area where the electrodes are located. However, the reactive species and the biological effects produced by the both plasma device types are quite similar. The factors produced by the plasmas include reactive oxygen species (ROS), reactive nitrogen species (RNS), ultraviolet (UV), as well as charged ions and electrons (Kong et al., 2009).

ROS such as OH and O could disrupt cells from the cell membrane to the inner nucleus through oxidation, which results in the effective inactivation of bacteria, fungi and viruses, or even programmed death of cancer cells (Dobrynin et al., 2009; Imlay et al., 1988; Lu et al., 2008b; Xiong et al., 2011). Non-thermal atmospheric-pressure plasmas can also enhance endothelial cell proliferation (Kalghatgi et al., 2010). These effects can be achieved by optimizing the treatment conditions such as the plasma parameters, working gases, and treatment time, which affect the dose of energy exposure, which in turn determine cell fate and behavior

(Dobrynin et al., 2009). A unique feature of the MPJs is that these plasmas typically have plasma spots of the order of ~10–100 μm and can be used for single-cell-level treatment (Kim et al., 2011).

This study demonstrates that treatment of murine NSCs with nanosecond microplasma bullets produced by MPJs induces and enhances their differentiation into a neuronal lineage, with a high selectivity of at least 75%. It is shown that the differentiated cells are mature and are mostly cholinergic and motor neuronal cells. The differentiated cell fate and lineages are identified by immunofluorescence microscopy, qRT-PCR, and Western Blot assay analyses. The term "selectivity" here refers to the preferential fate choice of the cells rather than the commonly used selectivity between different cell types. This proof-of-concept study is also extended to primary rat NSCs to show that MPJ agitation of stem cells may be quite a generic phenomenon and may potentially induce similar effects in other types of stem cells.

## Results and discussion

### MPJ enhances differentiation of neural stem cells

C17.2 NSC cell cultures were exposed to MPJs as shown in Figs. 1a,b. High-speed, nanosecond-resolution photography reveals that the plasma plume represents a train of fast-moving micro-bullet-like plasmas (Fig. 1c). To quantify NSCs differentiation, cell culture substrate was divided into 3 zones as shown in Supplementary Fig. S2. Zone A with a diameter of 3 mm, where cells were directly exposed to the plasma resulted in cells dispersion due to gas flow (Fig. 2b); zone B with a diameter of 18 mm, where the cells exposed indirectly showed significant cell differentiation after 48 h of the plasma treatment (Fig. 2c) compared to control untreated cells (Fig. 2a), while zone C (outer edges) showed no plasma effect (data not shown).

The results in Fig. 2 also showed that the plasma treatment altered the cell morphology with clear neurites and cell body extensions appearing after the exposure. Some neurites were longer compared to cell body extensions. This shows that differentiated cells are more mature and longer compared to undifferentiated NSCs. All these observations indicate that the plasma treatment enhances the differentiation of C17.2-NSCs.

The differentiation rates of NSCs on the 2nd, 4th and 6th days after the plasma treatment were determined as shown in Fig. 3. In the control group, only 7.33 ± 0.8% cells differentiated, which is 4 times less than after the plasma treatment. Four days later, the differentiation rates are 28.74 ± 1.05% and 77.3 ± 5.26% for the control and the plasma treated group in zone B, respectively. On day 6, the differentiation rate in the control group was 55.86 ± 2.74%, while more than 90% cells differentiated in the plasma-treated group. These experimental results show that the plasma treatment significantly enhances the differentiation of C17.2-NSCs.

### Characterization of plasma-induced NSCs differentiated cell lineages

NSCs are functionally characterized as cells with the capacity to proliferate, self-renew, and produce populous progeny that can differentiate into neurons, astrocytes and oligodendrocytes (Borrell and Reillo, 2012; Chojnacki et al., 2012; Rossi and Cattaneo, 2002). The microplasma treatment altered the NSCs morphology and significantly enhanced cell differentiation as shown above. The next step is to identify the specific types of cells produced from NSCs after the plasma exposure.

Immunofluorescence assay was used to identify different cell lineages. With the changes in protein expression profiles, NSCs can differentiate into three different cell types, as neurons, astrocytes and oligodendrocytes. Specific markers were chosen to define specific cell lineages. Nestin, a class VI intermediate filament protein which is highly expressed in NSCs and does not express in differentiated cells, has been utilized as a biological marker to identify undifferentiated NSCs (Kronenberg et al., 2003; Lendahl et al., 1990). β-Tubulin III, a cytoskeletal protein whose expression increases during axonal outgrowth, is expressed exclusively by neurons and considered a specific marker for neurons (Lee et al., 1990). Glial fibrillary acidic protein (GFAP), which is thought to help in maintaining astrocyte mechanical strength and the shape of cells, is primarily expressed by astrocytes specifically (Goss et al., 1991). Adenomatous polyposis coli (APC) is primarily expressed by oligodendrocyte cells and used as an oligodendrocyte marker. Oligodendrocyte marker O4 persists in immature oligodendrocytes and is commonly used as the earliest recognized marker specific for the oligodendroglial lineage (Bansal et al., 1989; Ono et al., 1997; Sommer and Schachner, 1981).

Immunofluorescent results (Fig. 4a) showed that the 60 s plasma treated C17.2-NSCs cultured for 6 days after the plasma exposure presented differential expression patterns for protein markers which indicated various cell lineages. Protein expression for nestin (+, green) which is a biomarker for NSCs, decreased; β-Tubulin III (+, red) which is a neuron marker, significantly increased; O4 (+, green) as an oligodendrocyte marker slightly increased; and GFAP (+, red) as an astrocyte marker remained unchanged compared to control groups. Statistical data analysis of three-directional differentiation of C17.2-NSCs was performed across 8 randomly selected view-fields of tested samples by using Image-Pro Plus software (Fig. 4b).

Most of the C17.2 cells differentiated into neuronal lineage (~75%) in the 60 s plasma treated group compared with ~35% in the control group. However, in the other two differentiation lineages, the amount of oligodendrocytes was low (less than 1% in the control group) and increased to ~8% in the 60 s plasma treated group; the abundance of astrocytes (~18%) with or without the plasma treatment has not changed. From Fig. 4 it is clearly seen that the extensions of the cells treated with the plasma are much longer compared to the untreated and gas-flow exposed samples. Moreover, the number of cells that produce the extensions is clearly much larger in the plasma-treated sample which is clearly seen by comparing the neutral gas flow treated and the plasma-treated samples.

### NSCs differentiation rates and morphological analysis

C17.2-NSCs differentiated into bipolar or multi-polar neurons with long neurites and extended cell body after the plasma treatment compared to short neurites in control untreated cells (Fig. 4a). The observed dense connections

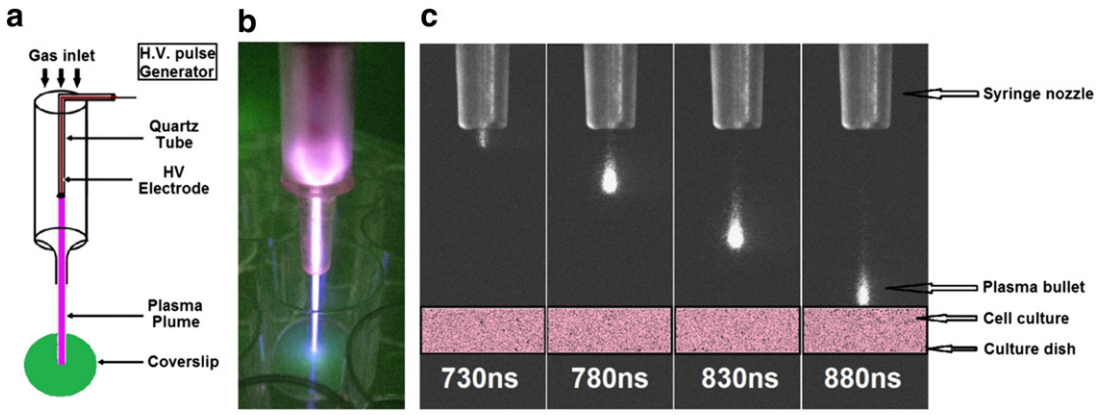


**Figure 1** Atmospheric-pressure microplasmas used in the regulation of differentiation of neural stem cells. (a) Schematic of the experimental set-up; (b) Photograph of the plasma jet impacting on NSCs; (c) High-speed photographs of the microplasma bullet propagating to cells in the culture dish taken by a high-speed ICCD camera from the syringe nozzle.

between neurons by outgrown neurites suggest the formation of a three-dimensional neural network. Morphological analysis of neurons in the untreated control and the plasma treated groups showed significant differences in the dendritic area (Fig. 5a), number of primary dendrites (Fig. 5b) and neurite length (Fig. 5c) of the neurons. These results demonstrate that the average dendritic area increased from ~300 $\mu m^2$ to 800 $\mu m^2$, the number of primary dendrites increased up to 3 times whereas the length of neurites increased from ~160 $\mu m$ to 280 $\mu m$. These data confirm that the plasma treatment effectively induces selective neuronal differentiation of NSCs.

## Identification of specific neural lineages biomarkers after the plasma exposure

To confirm specific neural cell lineages, quantitative PCR and immunoblotting assays were used to measure gene expression after the plasma treatment. Nestin, β-Tubulin III, GFAP and Olig2 genes were quantified by qRT-PCR after 2, 4, and 6 days of the plasma treatment. The results showed that the plasma exposure down-regulated Nestin expression which means that the number of undifferentiated NSCs is much less compared to the untreated control group (Fig. 6a). However, the plasma treatment upregulated the gene expression for β-Tubulin III (Fig. 6b) and Olig2 (Fig. 6d) which are biomarkers for neurons and oligodendrocytes; this indicates the effective differentiation of NSCs into neurons and oligodendrocytes. Olig2 expression after the plasma treatment showed different variations with respect to the control sample at 2 days and 4/6 days. GFAP expression was not affected after the plasma treatment (Fig. 6c).

We further confirmed our qRT-PCR gene expression results by Western Blot analysis (Fig. 7) to measure protein levels of specific neuronal biomarkers after the plasma treatment. The plasma exposure reduced Nestin protein expression, upregulated β-Tubulin III and APC which confirmed the enhanced NSCs differentiation into neurons and oligodendrocytes after the plasma treatment. Similarly as observed in qRT-PCR, protein expression for GFAP was not affected after the plasma exposure. These results determine that the plasma exposure enhances the differentiation of NSCs into neurons and oligodendrocytes.

## Possible role of reactive plasma species

MPJs produce various reactive agents, including charged species (*e.g.*, positive or negative ions), ROS (O, $O_2^*$, $OH^*$, etc.), and nitric oxide (NO). These active species have different biological functions and mechanisms to interact with bacteria, fungi, viruses, cancer cells and tissues and are also implicated in nanoscale synthesis in reactive plasmas (Dobrynin et al., 2009; Kogelschatz, 2003; Laroussi, 2005; Walsh et al., 2006). To

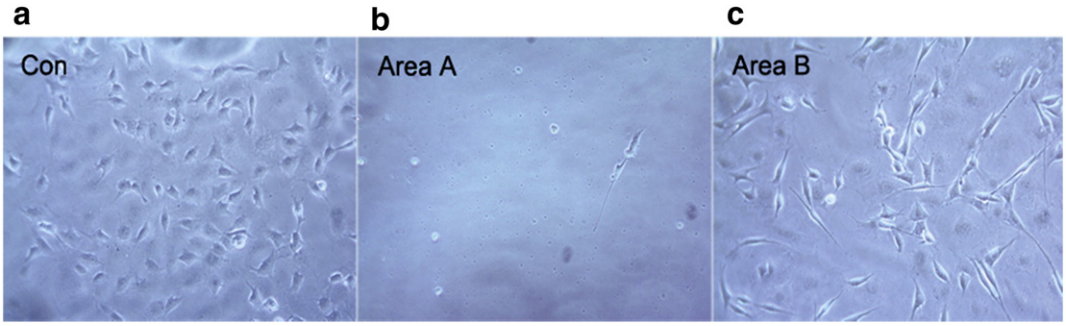


**Figure 2** Ordinary inverted phase contrast light microscope images of the cell differentiation after 2 days culture. (a) Control group; (b) area A in the plasma-treated group; (c) area B in 60 s plasma-treated group.

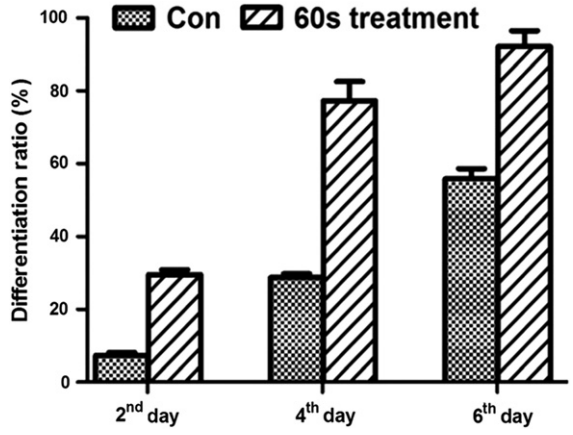


**Figure 3** Differentiation rate of the cells for the control group and the 60 s plasma-treated group in zone B after two, four, and six days culture.

identify the active factor involved in the plasma induced NSCs differentiation, active species in the plasma plume were measured. A typical optical emission spectrum from 200 nm to 800 nm of the plasma plume shows He and NO, and excited O, OH, $N_2$, $N_2^+$ (Supplementary Fig. S3) species. The plasma bullet contains excited and long-living species that may serve as active factors for NSC differentiation. In particular, biologically-relevant NO species were detected in the 200–300 nm spectral range (Yan et al., 2012).

Optical emission spectrum shows that the microplasma generates OH, O, NO and other reactive species. The reactive oxygen species (ROS) are generated through

$$He* + O_2 \rightarrow He + O_2^+ + e \quad (1)$$

$$He^+ + O_2 \rightarrow He + O^+ + O \quad (2)$$

$$O_2^+ + e \rightarrow 2O \quad (3)$$

$$O + H_2O \rightarrow 2OH \quad (4)$$

Atomic oxygen (O) is hard to dissolve in liquids, so it cannot directly react with the C17.2-NSCs as the cells are in the culture medium. The characteristic time of reaction (4) that generates OH species can be estimated to be as long as 6 s (Liu et al., 2010; Waskoenig et al., 2010). Presumably, O only plays an indirect role in induction of C17.2-NSCs differentiation. However, O could react with $N_2$ to produce NO, which can dissolve in liquids and may be an active factor responsible for NSCs differentiation.

As a neurotransmitter, NO has been previously shown to regulate NSCs proliferation and differentiation (Bansal et al., 1989; Boulu et al., 1994; Calabrese et al., 2007; Cheng et al., 2003). Exogenous NO is also implicated in neuronal differentiation, proliferation, and axonal growth (Arnhold et al., 2002). Moreover, previous measurements demonstrated that the plasma treatment increases both the extra- and intra-cellular NO concentration (Yan et al., 2012). The results of this work show that after 60 s of the plasma treatment, concentration of NO increased in the cell culture medium (Supplementary Fig. S4a). Additionally, we observed that intracellular NO levels also increased after the plasma treatment (Supplementary Fig. S4b).

We have also ascertained that NO species in general (*e.g.*, produced by other means) exert a quite similar effect on the cells. These results have been obtained by selectively adding NO donors (SNP) and NO scavengers (Hgb) to the cell medium, untreated, treated with gas flow, and plasma treated, to obtain a systematic picture of the effect of NO species. The results summarized in Supplementary Fig. S5 suggest that the effects of the microplasma and NO donors (SNP) appear to be quite similar and both lead not only to the enhanced neuronal differentiation but also to the enhanced maturity of the neuronal cells, as evidenced by markedly stronger up-regulation of both β-Tubulin III and NF200.

These experiments support our conclusion that microplasma-generated NO species are indeed important factors in inducing stem cell differentiation. Essentially, the differentiation of NSCs is mediated by related gene expression/regulation (Liste et al., 2007). Thus, our experimental data indicate that NO may indeed be an active factor produced by the plasma to promote the NSC differentiation *via* stimulating related gene expression/regulation. Further research is required to explore specific mechanisms of the effect of other plasma-generated reactive species to induce NSCs differentiation which in turn can be used for nervous system disorder treatments.

## Neuronal fate specification

We have also used combinatorial immunofluorescence and Western Blot analyses to determine if the differentiated neural cells mature and also to identify what specific types of neuronal cells emerge as a result of the microplasma agitation. Different biological markers were used, such as NF200 (for mature neurons), ChAT (for cholinergic neurons), LHX3 (for motor neurons), GABA (for GABAergic neurons), Serotonin (for serotonergic neurons), and TH (for dopaminergic neurons). These results are summarized in Fig. 8. The immunofluorescence studies (Fig. 8a) suggest that large numbers of mature neurons, cholinergic and motor neurons appear in the plasma-treated group. Furthermore, GABAergic and serotonergic neurons were rarely seen in the images, whereas no dopaminergic neurons were detected. These results were cross-referenced by the Western Blot analysis of the expression of NF200, ChAT and LHX3 biomarkers presented in Fig. 8b. These results show a strong up-regulation of the expression of all these 3 markers, consistently with the immunofluorescence imaging results in Fig. 8a. This indicates that the plasma treatment promoted the maturation of the differentiated neurons as well as the preferential differentiation of the NSCs into cholinergic and motor neurons. However, because LHX3 is also a biomarker of interneurons, we have conducted the additional test using a more specific marker Hb9 of the motor neurons (Thaler et al., 2002), see Fig. 8b. One can clearly see a strong expression of Hb9 in the plasma-treated group, which further confirms the effective formation of motor neurons as a result of the microplasma treatment.

## Study of MPJ effect on primary rat NSCs

To show that the observed microplasma effects could potentially be generic and applicable to other neural progenitor cells, we have studied the effect of MPJs on primary rat NSCs. These

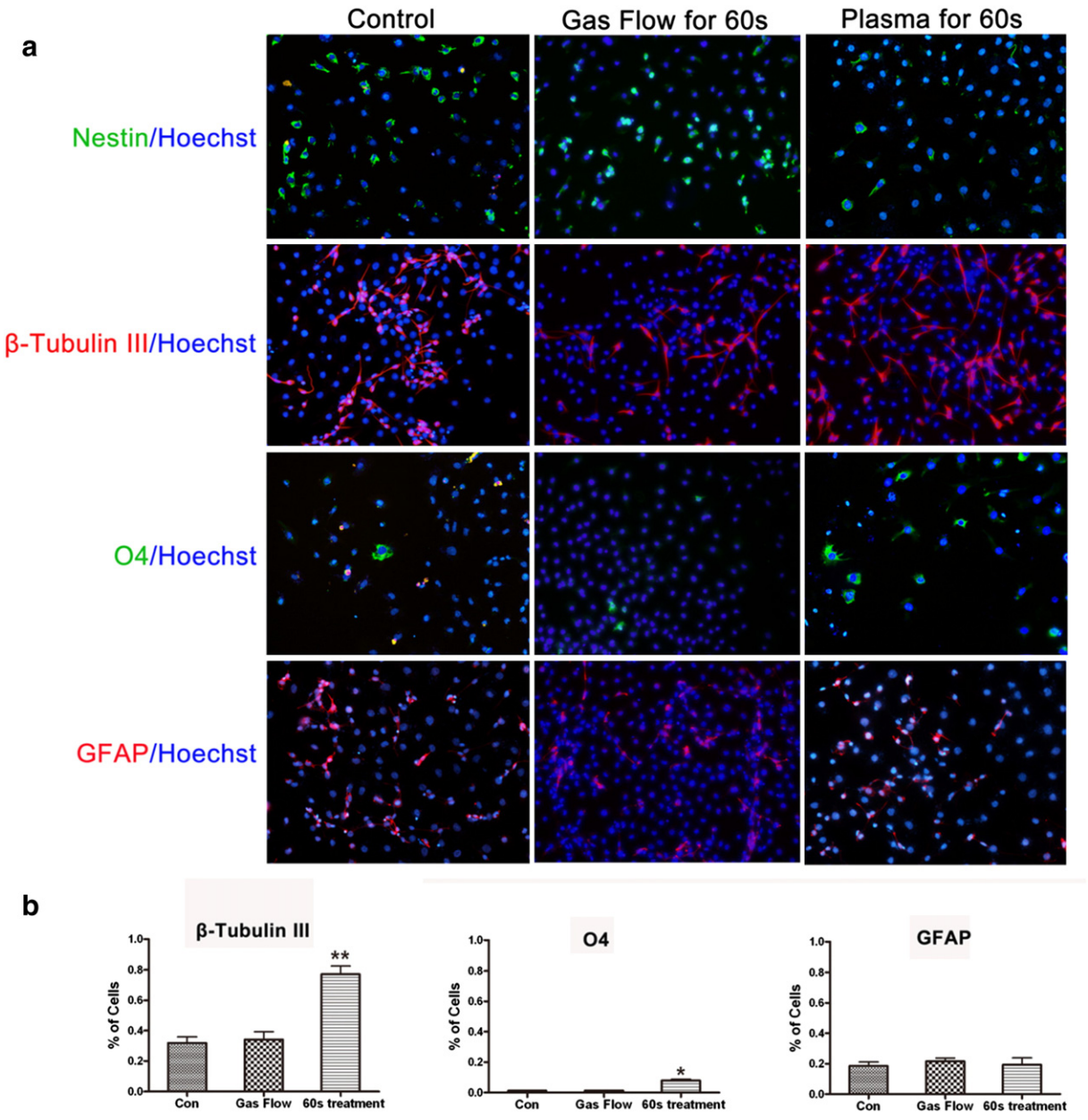


**Figure 4** (a) Immunofluorescence detection of C17.2-NSCs untreated (left), gas flow with no plasma (middle), and 60 s plasma-treated (right) for 6 days culture. Nestin (+, Green)/Hoechst; β-Tubulin III (+, Red)/Hoechst; O4 (+, Green)/Hoechst; GFAP (+, Red)/Hoechst. Blue nuclear counter stain is Hoechst 33258. (b) Bar charts of the percentage of differentiated cells in the control, gas flow and 60 s plasma-treated group after 6 days culture.

results are summarized in Fig. 9. Very similar procedures were followed for this type of cells. From Fig. 9b, it follows that about 95% of untreated cells showed a strong expression of Nestin biomarker, indicating that the NSCs were in an appropriate undifferentiated condition before the microplasma exposure. The gas flow did not induce any significant morphological changes, while the MPJ treatment led to the very significant changes evidenced by the pronounced neurite branching and outgrowth, as can be clearly seen in Fig. 9c. Moreover, the neurite length was much larger in the microplasma-treated samples. These results are consistent with the immunofluorescence studies of the expression of β-Tubulin III and O4 biomarkers specific to the neuronal and oligodendrocytal lineages, respectively. The results in Fig. 9d clearly show a much stronger branching and the emergence of much longer neurites in the plasma-treated samples. Likewise, the expression of O4 indicates the development of the oligodendrocytal progeny. These results suggest that the MPJ exposure also induces a qualitatively similar effect on another type of neural progenitors.

The results of quantitative image analysis of the rat NSC differentiation are shown in Fig. 10. It is clearly seen that in the plasma-treated group, the percentage of undifferentiated cells becomes much smaller (Fig. 10a) while the number of neurons

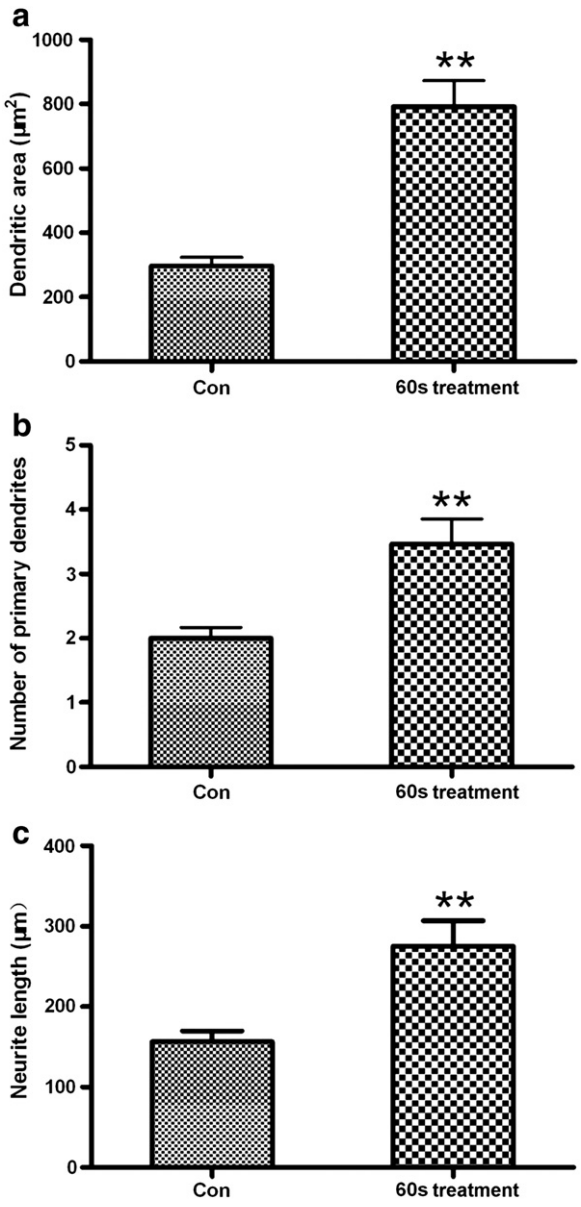


**Figure 5** Bar chart of the neuronal morphology analysis in the control and the 60 s plasma-treated group after 6 days culture. (a) Dendritic area; (b) Number of primary dendrites; (c) Neurite length.

(Fig. 10b) and oligodendrocytes (Fig. 10c) much increases. The average neurite length of the plasma-treated rat NSCs is also nearly two times larger compared to the control sample (Fig. 10d). Therefore, there is a possibility that the process conditions may be adjusted to optimize the quantitative MPJ effects on the primary rat NSCs, as well as possibly extended to other types of neural progenitor cells.

## Conclusion

Therefore, atmospheric-pressure plasma exposure represents a promising new approach towards highly-controlled NSCs differentiation to be utilized in various medical treatments of human neurological disorders and injuries of the CNS. This study showed that the atmospheric-pressure microplasma treatment produced neurons with long neurites and extended cell bodies. The quantized microplasma bullets of nanosecond duration significantly increased the differentiation rates compared to un-treated control neural stem cells. Our experimental data from immunofluorescence, qRT-PCR, and immunoblotting showed that the plasma-induced C17.2-NSCs differentiation was predominately towards a neuronal lineage (~75%), also accompanied by an increased population of oligodendroglial lineage. The cell fate specification study identified that the differentiated cells matured and preferentially produced cholinergic and motor neurons. Importantly, a quite similar effect was demonstrated using another type of neural progenitors, namely, primary rat NSCs.

Finally, this study demonstrates that atmospheric-pressure microplasmas represent an effective and safe tool for the differentiation of the NSCs selectively into neuronal lineage. Moreover, this finding may potentially be quite generic and possibly used to induce effective and selective differentiation of other types of neural progenitor cells. Further studies in this direction are therefore highly warranted.

## Materials and methods

### Cell Culture

Murine immortalized neural stem cell line C17.2 (C17.2-NSC, cell line identification is shown in Supplementary Fig. S1) (Snyder et al., 1992), were maintained in Dulbecco's modified Eagle medium (DMEM, Gibco BRL, Grand Island, NY) supplemented with 10% fetal bovine serum (FBS), 5% horse serum (HS) and 1% penicillin/streptomycin (Hyclone, Logan, UT) in a humidified atmosphere of 5% $CO_2$ and 95% air at 37 °C. The logarithmic phase C17.2-NSC cells were detached by trypsin and planted into a 12-well plate with the density of ~2 × $10^4$ cells/ml. Following cell attachment, the cells were washed twice with serum-free DMEM and cultured in differentiation medium consisting of DMEM/F-12 (Hyclone, Logan, UT) with 1% N-2 supplement (Gibco BRL, Grand Island, NY, USA) for 48 h before plasma treatment. In the immunofluorescence experiment, cells were seeded on 20 mm (diameter) poly-D-lysine (Sigma Chemical Co., St. Louis, MO, USA) coated glass coverslips in the 12-well plate with differentiation medium. Sham-treated controls were kept in differentiation medium at room temperature during the experimental procedure to ensure uniform treatment conditions.

Primary rat neural stem cells were isolated from the hippocampus of post-natal (P0–P1) SD rats according to methods described previously (Hu et al., 2004). The neurospheres derived from primary NSCs were maintained in OriCell™ Sprague–Dawley (SD) Rat Neural Stem Cell Growth Medium (Cyagen, USA) on uncoated T25-flasks (Corning). All the experiments were performed with cells that had undergone two passages. For the differentiation of Rat NSCs, neurospheres were seeded onto poly-D-lysine coated coverslips in the 12-well plate with differentiation medium, which consists of DMEM/F12, 2% B-27 (Gibco) and 1% FBS.

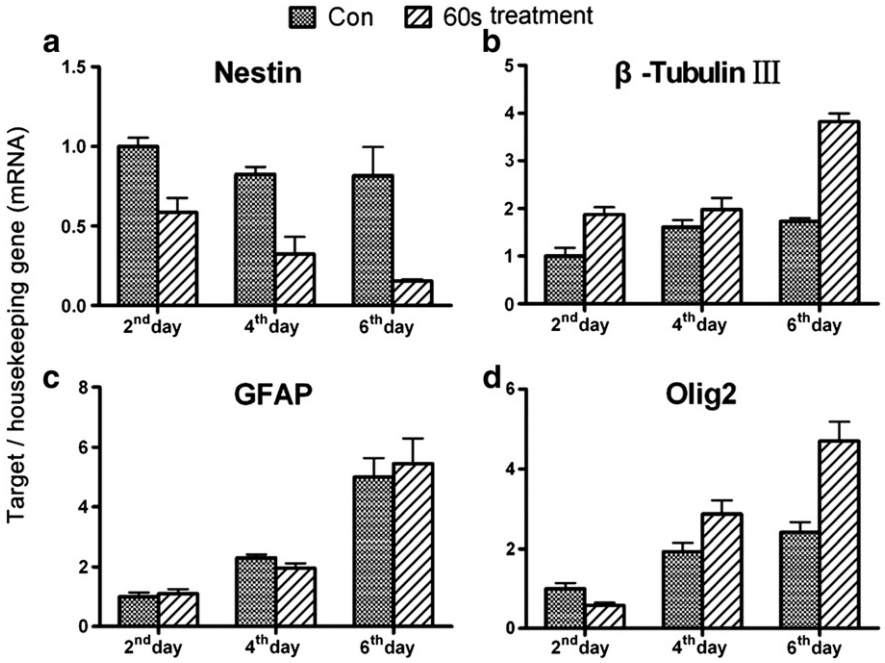


**Figure 6** Relative gene expression of mRNA level analysis by qRT-PCR of untreated and 60 s plasma-treated cells. (a) Nestin; (b) β-Tubulin III; (c) GFAP; (d) Olig2.

### *In vitro* microplasma cell treatment

A single-electrode atmospheric pressure room-temperature plasma jet device was used to treat the neural stem cells as shown in Fig. 1. More details about the MPJ device can be found elsewhere (Lu et al., 2008a). The device was driven by a pulsed power supply with a pulse rising time of 60 ns, pulse repetition frequency up to 10 kHz, pulse width variable from 200 ns to DC and voltage up to 10 kV. A mixture of working He and $O_2$ (1%) gases with the flow rate of 1 l/min was used. The pulse frequency, pulse width, and the amplitude of the applied voltage were fixed at 8 kHz, 1.6 μs, and 8 kV, respectively. Total 12 samples were divided into two groups, the control group, and the 60 s plasma treatment group. Each group contains six samples. The distance between the nozzle of the syringe and the cell well hole was 15 mm. After the plasma treatment, 1 ml new differentiation medium was added into each hole to replace the original culture, and then incubated in a humidified atmosphere of 5% $CO_2$ and 95% air at 37 °C. Two types of control groups were used, namely untreated cells and cells treated with only the He and $O_2$ (1%) gas flow, without the plasma generation; these results are shown separately where appropriate. This is used to show that the effect of the gas flow alone is much weaker compared with the plasma effect. In principle, gas flows may affect stem cell differentiation, potentially through biochemical, thermal, and mechanical agitation factors. The helium gas is inert hence the biochemical pathway is unlikely. A similar conclusion holds for the thermal pathway because the temperature of the plasma jet is close to ambient conditions of experiments. Typical velocities of gas atoms/molecules in the gas flow ("wind") are just about 10 m/s which is comparable with a typical sea breeze speed. This gentle gas flow is very unlikely to generate the levels of mechanical stress which is used for mechanical agitation of stem cells. Therefore, pure mechanical agitation by the near-room-temperature gas flow is unlikely, which is consistent with our observations. More details about the microplasma jet device, different zones in the samples affected by the treatment and the optical emission spectra generated by the MPJs can be found in Supplementary Sections S2, S3, and S5.

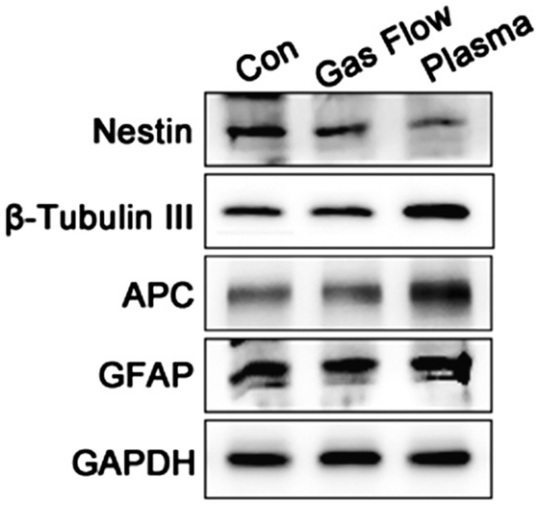


**Figure 7** Western Blot analysis of nestin, β-Tubulin III, APC, GFAP, and GAPDH expression in C17.2-NSCs in the control group, the gas flow with no plasma group, and the 60 s plasma-treated group after 6 days culture.

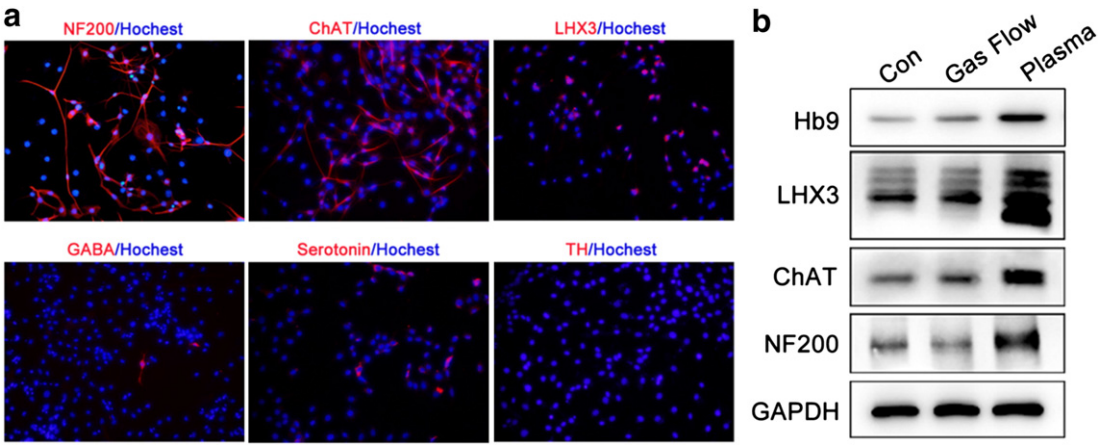


**Figure 8** Neuronal fate specification studied by (a) immunofluorescence and (b) Western Blot analyses. Strong expression of NF200, ChAT, and LHX3 biomarkers of the mature, cholinergic, and motor neurons, respectively is confirmed for the plasma-treated group by the results of the both analyses. Additional Western Blot test using Hb9 biomarker specifically confirms the formation of motor neurons in the plasma-treated group (B).

## Cell morphology analysis

To assess morphological changes in NSCs following the plasma treatment, the plates were examined with an inverted phase contrast light microscope (XD-202, Nanjing Jiangnan Novel Optics Co., Ltd) and photos were taken every day. In order to compare the differentiation rate of the control group and the plasma treated group in zone B, eight different visual fields were picked randomly for each sample every other day. The total number of cells and the number of differentiated cells in each visual field were counted. The cell with one or more neurites was considered differentiated. The differentiation rates on the 2nd, 4th, and 6th days were then calculated according to the number of differentiated cells *versus* the total number of cells.

## Immunofluorescence and quantification

Cells were seeded on 20 mm (diameter) poly-D-lysine coated coverslips for immunofluoresence analysis. Samples were fixed with 4% paraformaldehyde (Beyotime, Jiangsu, China) for 20 min followed by permeabilization with 0.2% TritonX-100 in PBS for 10 min at room temperature. The cells were then washed three times with PBS and incubated in 10% goat serum for 1 h to block any non-specific interactions. Then the samples were incubated with primary antibody at 4 °C overnight. The following antibodies were used to detect antigens: mouse anti-nestin (Beyotime, Jiangsu, China), rabbit anti-β-Tubulin III (Sigma Aldrich, USA), rabbit anti-GFAP (Dako, Denmark), and mouse anti-O4 (R&D Systems, USA), rabbit anti-NF200 (Sigma), rabbit anti-ChAT (Sigma), rabbit anti-LHX3 (Sigma), rabbit anti-Tyrosine Hydroxylase (Abcam, Cambridge, MA), rabbit anti-GABA (Sigma), rabbit anti-serotonin (Abcam, Cambridge, MA). After washing with PBS, cells were further incubated with Cy3-conjugated or Alexa Fluor 488-conjuated secondary antibodies (Jackson Immuno Research, USA) for 1 h at room temperature. Hoechst 33258 (Beyotime, Jiangsu, China) staining was used to label nuclei. Finally, the samples were imaged using a Nikon fluorescent microscope (80i, Nikon, Tokyo, Japan). Images were combined in figures using Adobe Photoshop CS3. For the morphology analysis of neuron (β-Tubulin III+ cells) and quantification of the percentage of cells producing a given marker protein, at least 8 randomly selected fields were photographed in each testing sample and the numbers of positive cells were determined relative to the total number of Hoechst 33258-labelled nuclei using Image-Pro Plus software.

## Quantitative real-time PCR (qRT-PCR)

Cells were treated with or without plasmas and cultured for the indicated time points. Total RNA was extracted with the RNAprep pure Cell/Bacteria Kit (Tiangen Biotech, Beijing, China) according to the manufacturer's instructions. About 1.5 μg RNA from each treatment was reverse transcribed into cDNA, which was subsequently served as the template for qRT-PCR, using RevertAid first-strand cDNA synthesis kit (Fermentas, USA). The primers (Supplementary Table S1) for qRT-PCR were designed using Primer Express software. Using the SuperReal PreMix Plus (SYBR Green) reagents (Tiangen Biotech) combined with gene-specific primers, qRT-PCR was performed on a Bio-Rad CFX-96 detection system (Bio-Rad, Hercules, CA, USA) using three stage amplification program. The specificity and amplification efficiency of all primers for each genes were tested prior to qRT-PCR experiments. The amplification efficiencies for each gene were between 0.9 and 1.1 and the specificity was confirmed by the melting curve analysis that a single peak indicated that a single DNA sequence was amplified during PCR. A housekeeping gene (GAPDH) was used as the reference gene that served as a benchmark for normalization. Each sample was tested in triplicate, and the samples obtained from three independent experiments were used for the analysis. The differences in gene expression levels were calculated using the $2^{-\Delta\Delta Ct}$ method (Lendahl et al., 1990).

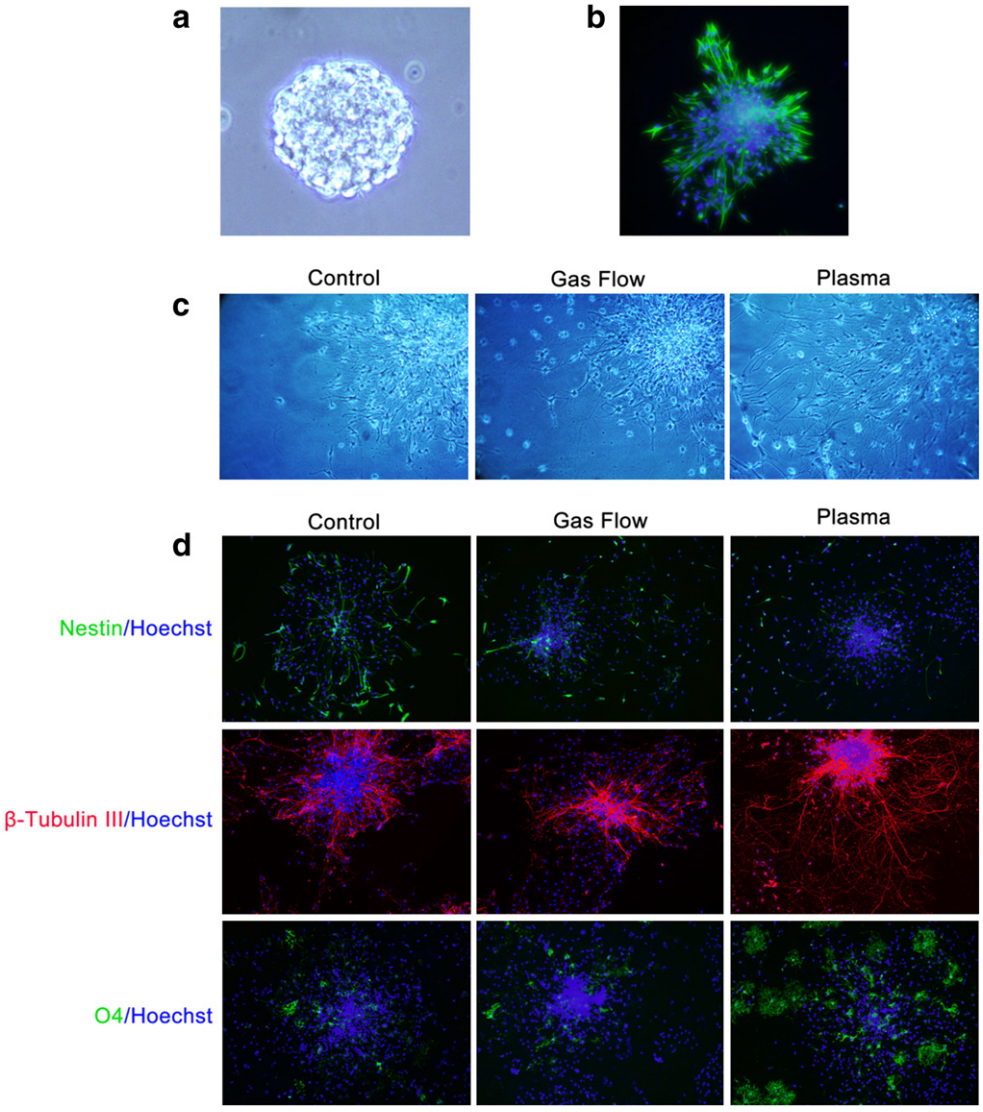


**Figure 9** Effect of MPJ exposure on the primary rat NSCs. a: Neurospheres in suspension culture. b: The primary state of the primary rat NSCs was undifferentiated as evidenced by the strong expression of Nestin NSC detected by immunofluorescence imaging. c: Observation of morphological changes following the $He/O_2$ gas and MPJ exposure shows the pronounced branching and elongation of neurites after the plasma treatment. d: Immunofluorescence for the specific neural lineage biomarkers. The expression of β-Tubulin III and O4 biomarkers is much stronger in the plasma treated group compared to the untreated and gas flow treated groups. The MPJ exposure strongly promotes the differentiation of the primary Rat NSCs into the neuronal and oligodendrocytal progeny.

## Western Blot analysis

After the plasma treatment, cells were cultured for 6 days and then harvested in lysis buffer (Beyotime, Jiangsu, China) in the presence of protease inhibitor PMSF (Beyotime, Jiangsu, China) (Zhao et al., 2013). A quantity of 30 μg of total cellular proteins per lane was separated on 10% sodium dodecyl sulfate-polyacryl amide gel electrophoresis (SDS-PAGE) and transferred onto nitrocellulose membrane. After blocking with 5% nonfat dried milk, the membranes were incubated with the antibodies against nestin (SantaCruz, CA), β-Tubulin III, GFAP, APC (SantaCruz), Hb9 (Bioss, China), LHX3, NF200, ChAT, and GAPDH (SantaCruz). Horseradish peroxidase (HRP)-conjugated goat anti-mouse or goat anti-rabbit IgG (SantaCruz) were used to detect the primary antibodies above. Detection of transferred proteins (antigens) were performed with an enhanced chemiluminescence detection kits (Millipore, USA) using ChemiDocXRS + (Bio-Rad, USA). GAPDH was used as a control protein because its expression was the same for untreated samples, samples exposed to the gas flow only, and the plasma-treated samples, as can be seen in Figs. 7 and 8, as well as Supplementary Fig. S5.

## Microplasma diagnostics

A half meter spectrometer (Princeton Instruments Acton SpectraHub 2500i) is used to measure the optical emission spectra (OES) of the plasma plume by using a fiber to collect the light. The distance between the fiber end and the plasma plume is set at 15 mm. Plasma bullets, generated by

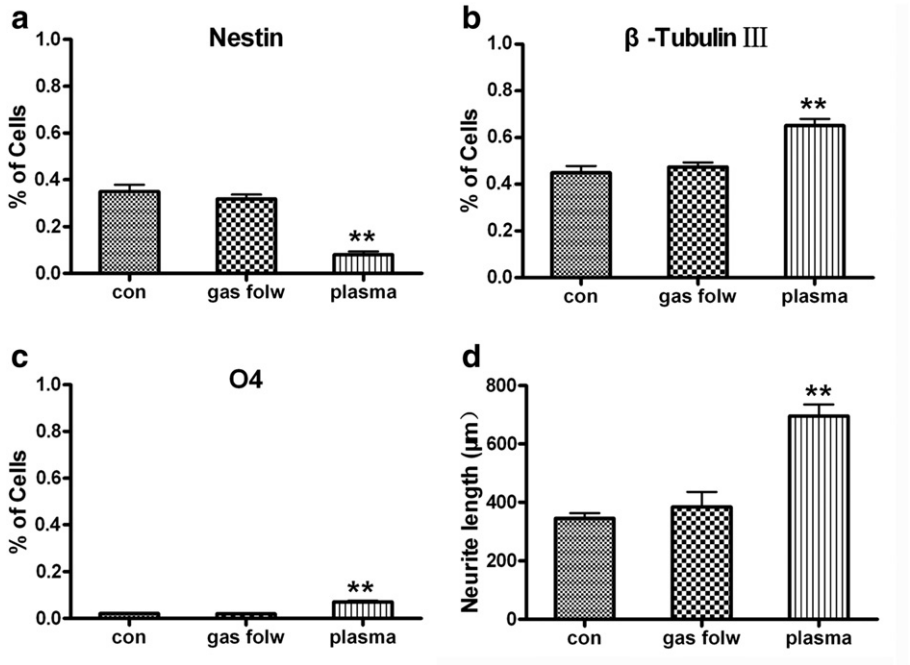


**Figure 10** Quantitative analysis of the differentiation of rat NSCs. (a) % of cells expressing Nestin+ (biomarker for undifferentiated NSCs); (b) % of cells expressing β-Tubulin III+ (biomarker for neurons); (c) % of cells expressing O4+ (biomarker for oligodendrocytes); (d) average neurite length of differentiated neurons. All the results are shown for the control, gas-flow-only, and plasma-treated groups.

the plasma device and propagated from the syringe nozzle to the C17.2-NSCs samples, were captured by a high-speed ICCD camera (PI-MAX2: 1003RB-FG-46, wavelength from 200 to 900 nm). The distance between the nozzle and the sample is set at 15 mm.

## Nitric oxide effect characterization

The extracellular and intracellular NO concentrations were determined using NO detection kit (Beyotime, Jiangsu, China) according to instructions provided by the manufacturer. For the detection of extracellular NO concentration, conditioned medium from C17.2-NSCs cultures after 6 days incubation was collected as samples for measurement. For the intracellular NO concentration determination, the cells cultured for 6 days after the plasma treatment were washed twice with ice-cold PBS after removing the medium, and then were lysed using cell lysis buffer (Beyotime, Jiangsu, China). The lysates were collected and centrifuged at 4 °C for 5 min. The supernatants were collected as samples to be tested. Assays were carried out in triplicate, and a standard curve using $NaNO_2$ was generated for each experiment for quantification. Briefly, 50 μl of samples or standard $NaNO_2$ were mixed with 50 μl of Griess reagent I and 50 μl of Griess reagent II in a 96-well plate at room temperature for 10 min. The absorbance was measured at 560 nm on a microplate reader (Sunrise, Tecan). NO concentration was calculated with a reference to a standard curve of $NaNO_2$ generated by known concentrations.

To ascertain that NO species may induce NSC differentiation, we have complemented the NO concentration measurements with the inverted phase contrast light microscope imaging and Western Blot analysis. C17.2-NSCs were divided into eight groups: non-treated control, $He/O_2$ gas flow (60 s), plasma (60 s), SNP (100 μM, NO donor), Hgb (20 μM, NO-scavenger), $He/O_2$ gas flow and Hgb co-treated group, plasma and Hgb co-treated group, SNP and Hgb co-treated group. As seen in Supplementary Fig. S5A, C17.2-NSCs with the plasma treatment showed similar differentiation effects as the SNP-treated group. Meanwhile, the NO-scavenger reduced the plasma-induced NSCs differentiation similarly in SNP treated NSCs (positive control). To study NO production in each group (Supplementary Fig. S5B), plasma-treated groups were detected immediately after the treatment. Likewise, SNP treated groups were detected 48 h after SNP were added (SNP can release NO slowly in the medium). The results of NO concentration measurements were consistent with the results of Western Blot analysis for the expression of neuronal markers β-Tubulin III and NF200 (Supplementary Fig. S5C), which both markedly up-regulated both in the plasma and the SNP treatment groups. However, these effects were attenuated by the Hgb NO scavenger.

## Statistical analysis

GraphPad Prism 5.0 software was used for statistical analysis. Results were expressed as the mean ± standard error of the *mean* (SEM) of triplicate samples and reproducibility was confirmed in at least three independent experiments. Student's t-tests were used to compare the two groups. Differences were considered significant at $P < 0.05$ or $P < 0.01$.

## Neuronal fate specification study

To study if the differentiated neurons develop into mature neurons as well as the specific neuron types generated, the following procedures were used. The C17.2-NSCs were treated with the microplasma for 60 s, and after a continuous

differentiation for 6 days, immunofluorescence studies were used to identify neuron subtype-specific markers, such as NF200 (mature neurons), ChAT (cholinergic neurons), Hb9 and LHX3 (motor neurons), GABA (GABAergic neurons), Serotonin (serotonergic neurons), and TH (dopaminergic neurons). Because NF200, ChAT, and LHX3 biomarkers showed very strong immunofluorescence responses in the plasma-treated C17.2-NSC cells (Fig. 8a), the expressions of the same biomarkers were also positively detected in the Western Blot analysis (Fig. 8b). The expression of Hb9 was studied in the Western Blot analysis to more specifically identify the development of motor neurons (Fig. 8b).

### Study of MPJ effect on primary rat NSCs

This proof-of-principle study basically followed similar approaches that were used for C17.2-NSCs and described above. Neurospheres were processed in suspension culture (Fig. 9a). The neurospheres were allowed to adhere on poly-D-lysine coated coverslips for 24 h. Immunofluorescence was used to detect the marker (Nestin) for NSCs (Fig. 9b). To observe the morphological changes (Fig. 9c) induced by the $He/O_2$ gas flow and the microplasma treatment, the neurospheres were seeded on poly-D-lysine coated coverslips for 24 h. Then, the gas flow and the plasma treatment (90 s) were performed, followed by differentiation for 4 days in differentiation medium (DMEM/F12 + 2% B-27 + 1% FBS). Immunofluorescence studies were used to identify the biomarkers for the specific neural lineages. A similar set of biomarkers was used as in the C17.2-NSCs case. The effect of the MPJ exposure on the primary rat NSCs was qualitatively similar to the C17.2-NSCs, with stronger development of the neuronal lineage accompanied by the larger presence of olygodendrocites. This effect was quantified in Fig. 10 using the analysis of the immunofluorescence images in Fig. 9 by using the Image Pro software.

## Acknowledgments

Fruitful discussions with Prof. D. Haylock are gratefully appreciated. This work was partially supported by the National Natural Science Foundation (Grant Nos. 51077063, 51277087), Research Fund for the Doctoral Program of Higher Education of China (20100142110005), Chang Jiang Scholars Program, Ministry of Education, People's Republic of China, in part by the National Science and Technology Major Project of China (2013ZX08002-004; 2013ZX08010-004), the National Natural Science Foundation of China (No. 30871524 and No. 31071403), the National Natural Science Foundation of Hubei, China (2010 CBD 02403), the Wuhan Science and Technology Project (201260523185) and the Fundamental Research Funds for the Central Universities (HUST: 2011TS150). Support from the Australian Research Council, CSIRO's Science Leadership Program, Advanced Materials and Transformational Biology TCPs is also acknowledged.

## Appendix A. Supplementary data

Supplementary data to this article can be found online at http://dx.doi.org/10.1016/j.scr.2013.11.003.

## References

Arnhold, S., Faßbender, A., Klinz, F.J., Kruttwig, K., Löhnig, B., Andressen, C., Addicks, K., 2002. NOS-II is involved in early differentiation of murine cortical, retinal and ES cell-derived neurons—an immunocytochemical and functional approach. Int. J. Dev. Neurosci. 20, 83–92.

Bansal, R., Warrington, A.E., Gard, A.L., Ranscht, B., Pfeiffer, S.E., 1989. Multiple and novel specificities of monoclonal antibodies O1, O4, and R-mAb used in the analysis of oligodendrocyte development. J. Neurosci. Res. 24, 548–557.

Barnett, S.C., 2004. Olfactory ensheathing cells: unique glial cell types? J. Neurotrauma 21, 375–382.

Bergmann, O., Frisén, J., 2013. Why adults need new brain cells. Science 340, 695–696.

Bjorklund, A., Lindvall, O., 2000. Cell replacement therapies for central nervous system disorders. Nat. Neurosci. 3, 537–544.

Borrell, V., Reillo, I., 2012. Emerging roles of neural stem cells in cerebral cortex development and evolution. Dev. Neurobiol. 72, 955–971.

Boulu, R.G., Plotkine, M., Buisson, A., 1994. Nitric oxide, a novel neurotransmitter in the brain. Ann. Pharm. Fr. 52.

Boyer, L.A., Lee, T.I., Cole, M.F., Johnstone, S.E., Levine, S.S., Zucker, J.P., Guenther, M.G., Kumar, R.M., Murray, H.L., Jenner, R.G., et al., 2005. Core transcriptional regulatory circuitry in human embryonic stem cells. Cell 122, 947–956.

Breunig, Joshua J., Haydar, Tarik F., Rakic, P., 2011. Neural stem cells: historical perspective and future prospects. Neuron 70, 614–625.

Calabrese, V., Mancuso, C., Calvani, M., Rizzarelli, E., Butterfield, D.A., Giuffrida Stella, A.M., 2007. Nitric oxide in the central nervous system: neuroprotection versus neurotoxicity. Nat. Rev. Neurosci. 8, 766–775.

Chambers, I., Colby, D., Robertson, M., Nichols, J., Lee, S., Tweedie, S., Smith, A., 2003. Functional expression cloning of nanog, a pluripotency sustaining factor in embryonic stem cells. Cell 113, 643–655.

Cheng, A., Wang, S., Cai, J., Rao, M.S., Mattson, M.P., 2003. Nitric oxide acts in a positive feedback loop with BDNF to regulate neural progenitor cell proliferation and differentiation in the mammalian brain. Dev. Biol. 258, 319–333.

Chojnacki, A., Cusulin, C., Weiss, S., 2012. Adult periventricular neural stem cells: outstanding progress and outstanding issues. Dev. Neurobiol. 72, 972–989.

Dobrynin, D., Fridman, G., Friedman, G., Fridman, A., 2009. Physical and biological mechanisms of direct plasma interaction with living tissue. New J. Phys. 11, 115020.

Flanagan, L.A., Rebaza, L.M., Derzic, S., Schwartz, P.H., Monuki, E.S., 2006. Regulation of human neural precursor cells by laminin and integrins. J. Neurosci. Res. 83, 845–856.

Goss, J.R., Finch, C.E., Morgan, D.G., 1991. Age-related changes in glial fibrillary acidic protein mRNA in the mouse brain. Neurobiol. Aging 12, 165–170.

Grois, N.G., Favara, B.E., Mostbeck, G.H., Prayer, D., 1998. Central nervous system disease in langerhans cell histocytosis. Hematol. Oncol. Clin. North Am. 12, 287–305.

Hernández-Benítez, R., Ramos-Mandujano, G., Pasantes-Morales, H., 2012. Taurine stimulates proliferation and promotes neurogenesis of mouse adult cultured neural stem/progenitor cells. Stem Cell Res. 9, 24–34.

Hu, X., Jin, L., Feng, L., 2004. Erk1/2 but not PI3K pathway is required for neurotrophin 3-induced oligodendrocyte differentiation of post-natal neural stem cells. J. Neurochem. 90, 1339–1347.

Huang, Y.-J., Wu, H.-C., Tai, N.-H., Wang, T.-W., 2012. Carbon nanotube rope with electrical stimulation promotes the differentiation and maturity of neural stem cells. Small 8, 2869–2877.

Hwang, W.S., Ryu, Y.J., Park, J.H., Park, E.S., Lee, E.G., Koo, J.M., Jeon, H.Y., Lee, B.C., Kang, S.K., Kim, S.J., et al., 2004.

Evidence of a pluripotent human embryonic stem cell line derived from a cloned blastocyst. Science 303, 1669–1674.
Imlay, J., Chin, S., Linn, S., 1988. Toxic DNA damage by hydrogen peroxide through the Fenton reaction in vivo and in vitro. Science 240, 640–642.
Kalghatgi, S., Friedman, G., Fridman, A., Clyne, A., 2010. Endothelial cell proliferation is enhanced by low dose non-thermal plasma through fibroblast growth factor-2 release. Ann. Biomed. Eng. 38, 748–757.
Keidar, M., Walk, R., Shashurin, A., Srinivasan, P., Sandler, A., Dasgupta, S., Ravi, R., Guerrero-Preston, R., Trink, B., 2011. Cold plasma selectivity and the possibility of a paradigm shift in cancer therapy. Br. J. Cancer 105, 1295–1301.
Kim, J.Y., Kim, S.-O., Wei, Y., Li, J., 2010. A flexible cold microplasma jet using biocompatible dielectric tubes for cancer therapy. Appl. Phys. Lett. 96, 203701.
Kim, J.Y., Wei, Y.Z., Li, J.H., Foy, P., Hawkins, T., Ballato, J., Kim, S.O., 2011. Single-cell-level microplasma cancer therapy. Small 7, 2291–2295.
Kogelschatz, U., 2003. Dielectric-barrier discharges: their history, discharge physics, and industrial applications. Plasma Chem. Plasma Process. 23, 1–46.
Kolb, J.F., Mohamed, A.-A.H., Price, R.O., Swanson, R.J., Bowman, A., Chiavarini, R.L., Stacey, M., Schoenbach, K.H., 2008. Cold atmospheric pressure air plasma jet for medical applications. Appl. Phys. Lett. 92, 241501.
Kong, M.G., Kroesen, G., Morfill, G., Nosenko, T., Shimizu, T., van Dijk, J., Zimmermann, J.L., 2009. Plasma medicine: an introductory review. New J. Phys. 11, 115012.
Kronenberg, G., Reuter, K., Steiner, B., Brandt, M.D., Jessberger, S., Yamaguchi, M., Kempermann, G., 2003. Subpopulations of proliferating cells of the adult hippocampus respond differently to physiologic neurogenic stimuli. J. Comp. Neurol. 467, 455–463.
Laroussi, M., 1996. Sterilization of contaminated matter with an atmospheric pressure plasma. IEEE Trans. Plasma Sci. 24, 1188–1191.
Laroussi, M., 2005. Low temperature plasma-based sterilization: overview and state-of-the-art. Plasma Process. Polym. 2, 391–400.
Lee, M.K., Tuttle, J.B., Rebhun, L.I., Cleveland, D.W., Frankfurter, A., 1990. The expression and posttranslational modification of a neuron-specific β-tubulin isotype during chick embryogenesis. Cell Motil. Cytoskeleton 17, 118–132.
Lendahl, U., Zimmerman, L.B., McKay, R.D.G., 1990. CNS stem cells express a new class of intermediate filament protein. Cell 60, 585–595.
Liste, I., Garcia-Garcia, E., Bueno, C., Martinez-Serrano, A., 2007. Bcl-XL modulates the differentiation of immortalized human neural stem cells. Cell Death Differ. 14, 1880–1892.
Liu, D.X., Bruggeman, P., Iza, F., Rong, M.Z., Kong, M.G., 2010. Global model of low-temperature atmospheric-pressure He + $H_2O$ plasmas. Plasma Sources Sci. Technol. 19, 025018.
Lloyd, G., Friedman, G., Jafri, S., Schultz, G., Fridman, A., Harding, K., 2010. Gas plasma: medical uses and developments in wound care. Plasma Process. Polym. 7, 194–211.
Lu, X., Jiang, Z., Xiong, Q., Tang, Z., Pan, Y., 2008a. A single electrode room-temperature plasma jet device for biomedical applications. Appl. Phys. Lett. 92, 151504.
Lu, X., Ye, T., Cao, Y., Sun, Z., Xiong, Q., Tang, Z., Xiong, Z., Hu, J., Jiang, Z., Pan, Y., 2008b. The roles of the various plasma agents in the inactivation of bacteria. J. Appl. Phys. 104, 053309.
McKay, R., 1997. Stem cells in the central nervous system. Science 276, 66–71.
Okada, Y., Shimazaki, T., Sobue, G., Okano, H., 2004. Retinoic-acid-concentration-dependent acquisition of neural cell identity during in vitro differentiation of mouse embryonic stem cells. Dev. Biol. 275, 124–142.
Ono, K., Fujisawa, H., Hirano, S., Norita, M., Tsumori, T., Yasui, Y., 1997. Early development of the oligodendrocyte in the embryonic chick metencephalon. J. Neurosci. Res. 48, 212–225.
Ostrikov, K., Neyts, E.C., Meyyappan, M., 2013. Plasma nanoscience: from nano-solids in plasmas to nano-plasmas in solids. Adv. Phys. 62, 113–224.
Pellitteri, R., Spatuzza, M., Russo, A., Zaccheo, D., Stanzani, S., 2009. Olfactory ensheathing cells represent an optimal substrate for hippocampal neurons: an in vitro study. Int. J. Dev. Neurosci. 27, 453–458.
Reynolds, B., Weiss, S., 1992. Generation of neurons and astrocytes from isolated cells of the adult mammalian central nervous system. Science 255, 1707–1710.
Rodriguez, J.J., Olabarria, M., Chvatal, A., Verkhratsky, A., 2009. Astroglia in dementia and Alzheimer's disease. Cell Death Differ. 16, 378–385.
Rossi, F., Cattaneo, E., 2002. Neural stem cell therapy for neurological diseases: dreams and reality. Nat. Rev. Neurosci. 3, 401–409.
Shi, W., Wang, H., Pan, G., Geng, Y., Guo, Y., Pei, D., 2006. Regulation of the pluripotency marker Rex-1 by Nanog and Sox2. J. Biol. Chem. 281, 23319–23325.
Sleeper, E., Tamm, C., Frisen, J., Zhivotovsky, B., Orrenius, S., Ceccatelli, S., 2002. Cell death in adult neural stem cells. Cell Death Differ. 9, 1377–1378.
Snyder, E.Y., Deitcher, D.L., Walsh, C., Arnold-Aldea, S., Hartwieg, E.A., Cepko, C.L., 1992. Multipotent neural cell lines can engraft and participate in development of mouse cerebellum. Cell 68, 33–51.
Sommer, I., Schachner, M., 1981. Monoclonal antibodies (O1 to O4) to oligodendrocyte cell surfaces: an immunocytological study in the central nervous system. Dev. Biol. 83, 311–327.
Sunde, N., Zimmer, J., 1981. Transplantation of central nervous tissue. An intrduction with results and implications. Acta Neurol. Scand. 63, 323–335.
Temple, S., 2001. The development of neural stem cells. Nature 414, 112–117.
Thaler, J.P., Lee, S.K., Jurata, L.W., Gill, G.N., Pfaff, S.L., 2002. LIM factor Lhx3 contributes to the specification of motor neuron and interneuron identity through cell-type-specific protein–protein interactions. Cell 110, 237–249.
Walsh, J.L., Shi, J.J., Kong, M.G., 2006. Submicrosecond pulsed atmospheric glow discharges sustained without dielectric barriers at kilohertz frequencies. Appl. Phys. Lett. 89, 161505.
Wang, J.-H., Hung, C.-H., Young, T.-H., 2006a. Proliferation and differentiation of neural stem cells on lysine–alanine sequential polymer substrates. Biomaterials 27, 3441–3450.
Wang, J., Rao, S., Chu, J., Shen, X., Levasseur, D.N., Theunissen, T.W., Orkin, S.H., 2006b. A protein interaction network for pluripotency of embryonic stem cells. Nature 444, 364–368.
Waskoenig, J., Niemi, K., Knake, N., Graham, L.M., Reuter, S., Shulz-von der Gathen, V., Gans, T., 2010. Atomic oxygen formation in a radio-frequency driven micro-atmospheric pressure plasma jet. Plasma Sources Sci. Technol. 19, 045018.
Xiong, Z., Lu, X., Cao, Y., Ning, Q., Ostrikov, K., Lu, Y., Zhou, X., Liu, J., 2011. Room-temperature, atmospheric plasma needle reduces adenovirus gene expression in HEK 293A host cells. Appl. Phys. Lett. 99, 253703.
Yan, X., Xiong, Z., Zou, F., Zhao, S., Lu, X., Yang, G., He, G., Ostrikov, K., 2012. Plasma-Induced death of HepG2 cancer cells: intracellular effects of reactive species. Plasma Process. Polym. 9, 59–66.
Zhao, S., Xiong, Z., Mao, X., Meng, D., Lei, Q., Li, Y., Deng, P., Chen, M., Tu, M., Lu, X.P., Yang, G., He, G., 2013. Atmospheric pressure room temperature plasma jets facilitate oxidative and nitrative stress and lead to endoplasmic reticulum stress dependent apoptosis in HepG2 Cells. PLoS One 8, e73665.